

Microwave response of single crystal $\text{YBa}_2\text{Cu}_3\text{O}_{7-\delta}$ films as a probe for pairing symmetry

V.M. Pan, O.A. Kalenyuk, O.L. Kasatkin, and V.A. Komashko

*Institute for Metal Physics of the National Academy of Sciences of Ukraine
36 Vernadsky Blvd., Kiev 03142, Ukraine
E-mail: pan@imp.kiev.ua*

O.M. Ivanyuta and G.A. Melkov

T.G. Shevchenko National Kiev University, Radiophysics Faculty, 6 Glushkov Ave., Kiev 03127, Ukraine

Received October 31, 2005

Temperature dependences of the microwave surface impedance, $Z_s(T)$, are measured in the c -axis oriented single-crystal high- T_c superconducting cuprate $\text{YBa}_2\text{Cu}_3\text{O}_{7-\delta}$ (YBCO) thin films deposited by the off-axis dc magnetron sputtering onto CeO_2 -buffered single-crystal sapphire substrates (film thickness is $d \approx 150, 300, 480$ nm). Measurements are performed by a use of the coplanar resonator as well as the end-plate cylindrical cavity resonator techniques at a number of several discrete frequencies within the range of 5–134 GHz. The measurements have revealed unexpected peculiarities on the $Z_s(T)$ -dependences for the most perfect films under study. The peculiarities appear to be most strongly pronounced on the temperature dependences of the film surface resistance $R_s(T) = \text{Re}\{Z_s(T)\}$. The most important features of the unusual surface resistance behavior are: (i) the temperature dependence $R_s(T)$ of YBCO films under study at low temperatures obeys the exponential law: $R_s(T) = R_{\text{res}} + R_0 \exp[-\Delta_s/T]$ with the small energy gap Δ_s ($\Delta_s \approx 0.5T_c$ at $f = 5$ GHz); (ii) the most perfect films reveal a distinct two-peak structure of the $R_s(T)$ dependence with peaks positioned at 27–30 K and 48–51 K, while such peaks are not observed in less perfect films. The peaks are mostly pronounced at moderate (e.g. 34 GHz) frequencies and gradually disappear both at higher and lower frequencies, while their temperature positions remain unchanged. These features of perfect single-crystalline YBCO films are believed to reveal their intrinsic electron properties. Taking into account the possibility of a mixed ($s+id$)-type pairing symmetry as well as a significant role of extended out-of-plane crystal defects (such as dislocation lines or twin planes) in Bogolyubov's quasiparticle scattering within the most perfect YBCO films, one can suggest a consistent explanation for the anomalies observed in the $Z_s(T)$ behavior.

PACS: 74.25.Nf, 74.72.Bk, 74.78.Bz

Keywords: high- T_c , superconductivity, cuprate thin films, microwave surface impedance, pairing symmetry.

1. Introduction

Studies of microwave properties of high- T_c superconducting cuprates (HTS) are known to be one of the most effective and fruitful methods which provide rich information concerning electron properties and mechanisms of superconductivity in these materials. Measurements of the microwave surface impedance $Z_s(T, \omega) = R_s(T, \omega) + iX_s(T, \omega)$ of high quality HTS

single crystals or perfect single-crystalline films provide information on two general aspects of the superconducting state: the superfluid density and quasiparticle excitations from the condensate. Measurements of the imaginary part of the surface impedance $X_s(T, \omega)$ provide a direct measure of the penetration depth $\lambda(T)$, while measurements of the real part of the surface impedance $R_s(T)$ combined

with data on $\lambda(T)$ determine the real part σ_1 of the microwave conductivity $\sigma(T, \omega) = \sigma_1(T, \omega) - i\sigma_2(T, \omega)$, that in turn yield complementary information on the microscopic electronic properties of HTS, such as: low-energy quasiparticle excitations from the superfluid condensate, their scattering rate and density of states, the symmetry of Cooper pairing, etc. Numerous experimental and theoretical studies of microwave response, carried out during the last decade, revealed a lot of interesting features of the superconducting state in HTS metal-oxide compounds and partly shed light on the nature of superconductivity in these materials. For instance, the *d*-wave scenario of electron pairing symmetry in HTS is strongly supported by the data of microwave measurements [1–9]. However, all the features of the microwave response of HTS are not clear enough at present. In particular, it concerns a nature of the residual resistance, $R_{\text{res}}(\omega)$, microwave conductivity spectrum $\sigma(T, \omega)$, energy dependence of quasiparticles density of states and relaxation rate, a role of crystal defects of the different dimensionality and collective modes in quasiparticles scattering, etc. There are still a number of difficulties in understanding and explanation some experimental results on microwave properties of HTS cuprates in the framework of existing theoretical models [10–16].

One of the most pronounced peculiarities in microwave response of perfect single crystals and epitaxial thin films is nonmonotonous temperature dependence of the surface resistance, $R_s(T)$, observed up to now in different HTS cuprates. In particular, the temperature dependence $R_s(T)$ in $\text{YBa}_2\text{Cu}_3\text{O}_{7-\delta}$ (YBCO) perfect single crystals [1,3–5,7,8] and epitaxially grown single-crystalline thin films [2,6,17] experimentally observed by different groups, turned out to be nonmonotonous and revealed a pronounced peak at $T \leq T_c/2$. The temperature position and the height of the peak depend upon the frequency and crystal perfection. Such a peculiarity in $R_s(T)$ appears to be very sensitive to the crystal defect density. For instance, impurities (i.e., point defects) suppress the peak in $R_s(T)$ [1,17]. Analysis of the experimental data based on the phenomenological approach [4,7,18–22], assuming the Drude form of microwave conductivity for thermally excited quasiparticles $\sigma(T, \omega) = (n_q(T)e^2/m)[i\omega + 1/\tau]^{-1}$, sheds a light on the nature of observed broad peaks on $R_s(T)$ curves and explains also (at least qualitatively) its frequency dependence and suppression of the peak by impurities. This approach also allows one to extract the value of quasiparticle relaxation time $\tau(T)$ directly from microwave measurements of $R_s(T)$. It was demonstrated that $\tau(T)$ in perfect single crystals appears to be strongly increasing with the temperature reduction

and reaches the saturation value of order 10^{-10} – 10^{-11} s at low temperatures (below 20 K) [4,7].

In the present work $Z_s(T, \omega)$ dependences of perfect quasi-single-crystalline YBCO films deposited on CeO_2 buffered sapphire substrates are studied in order to establish relation between the microwave response and electron structure of the films under study, as well as their defect nanostructure. We have observed a distinct exponential type of $R_s(T)$ dependence at low temperatures for our films: $R_s(T) = R_{\text{res}} + R_0 \exp[-\Delta_s/T]$, characterized by a small gap value ($\Delta_s \sim 0.5T_c$), thus confirming the result of M. Hein *et al.* [23] for this sort of YBCO films. On the other hand, we demonstrate that for the most perfect epitaxially grown single-crystalline YBCO films the nonmonotonous character of $R_s(T)$ can be even more complicated than it was observed before: for such films our experiments have revealed two distinct rather narrow peaks on $R_s(T)$ curves, positioned at quite different temperatures: $T_1 = 27$ – 30 K and $T_2 = 48$ – 51 K [24]. This observation clearly indicates that the microscopic scenario of electron properties in HTS cuprates (like YBCO) is more intriguing and sophisticated, than it was assumed before. We suggest a theoretical explanation of observed results based on two main assumptions: (i) anisotropic (*s + id*) electron pairing; (ii) the dominant role of extended defects (*c*-axis aligned edge dislocations or twin planes) in the quasi-particle scattering. Such assumptions appear to be sufficient to explain the anomalous behavior observed in $Z_s(T, \omega)$ dependences and also to understand their difference from those, observed in single crystals as well as in other (less perfect) YBCO films.

2. Phenomenology of HTS cuprate microwave response (two-fluid model)

In the framework of a phenomenological approach in general the surface impedance of any superconductor can be described as (see, e.g., the review papers [3,18]):

$$Z_s(T, \omega) = R_s(T, \omega) + iX_s(T, \omega) = \left[\frac{i\mu_0\omega}{\sigma_1(T, \omega) - i\sigma_2(T, \omega)} \right]^{1/2}, \quad (1)$$

where R_s and X_s are the surface resistance and the surface reactance respectively; $\omega = 2\pi f$ – is the angular frequency; μ_0 – is the magnetic permeability of free space; σ_1 and σ_2 are the real and imaginary parts of ac conductivity. Accordingly to the two-fluid model of superconducting state, the components of ac conductivity are:

$$\sigma_1(T, \omega) = \frac{e^2}{m^*} n_N(T) \frac{\tau(T)}{1 + (\omega\tau(T))^2}, \quad (2)$$

$$\begin{aligned} \sigma_2(T, \omega) &= \frac{1}{\mu_0 \omega \lambda^2(T)} = \\ &= \frac{e^2}{m^* \omega} \left\{ n_S(T) + n_N(T) \frac{(\omega\tau(T))^2}{1 + (\omega\tau(T))^2} \right\}, \quad (3) \end{aligned}$$

where e and m^* are the electron charge and effective mass, respectively; n_N and n_S are densities of normal and superfluid carriers; τ is the relaxation time of normal carriers. The two-fluid model suggests that the following conservation law for densities $n_N(T)$ and $n_S(T)$ is hold:

$$n_N(T) + n_S(T) = n_0, \quad (4)$$

where n_0 is the density of carriers above T_c . The original two-fluid model, as well as its derivation from the microscopic theory, also suggests that all carriers become superconducting at $T = 0$ and $n_N(0) = 0$. Meanwhile, the numerous attempts of adjustment of the phenomenological two-fluid model description for experiments on microwave properties of HTS single crystals and thin films [18–23] led to the inevitable conclusion that there is some fraction of the unpaired normal carriers at $T = 0$, which are responsible for the residual surface resistance $R_{\text{res}} = R_s(T = 0)$, usually observed in experiments (especially in HTS cuprate thin films). Of course, these unpaired normal carriers most probably are spatially separated from the remaining superconducting part of material and concentrate near the surface or interface layer (or holes of order parameter in the film's interior). But in the framework of effective media theory to account this fraction of unpaired electrons at low temperatures it is usually assumed that the normal carriers density $n_N(T)$ in HTS cuprates is:

$$n_N(T) = n_{\text{res}} + (n_0 - n_{\text{res}})F(t), \quad (5)$$

where $t = T/T_c$ is the reduced temperature, and $F(t)$ is monotonously increasing function within the range $0 < t < 1$ with $F(0) = 0$ and $F(1) = 1$ (see e.g. [23]). In order to fit the experimental data usually one has to choose empirical $F(t)$ in a polynomial form, for instance: $F(t) = t^n$ with $n \geq 1$. This form is also consistent with a scenario of d -wave pairing, which predicts rather slow (quasi-linear) lessening of the normal quasiparticles density with a temperature decrease due to nodes in the gap function $\Delta(p)$ of d -wave superconductors [10]. Nevertheless, for some cases the best fitting of experimental data on $R_s(T)$ can be attained for other choice of function $F(t)$, e.g., an exponential one: $F(t) \sim \exp(-\delta/t)$. For

instance, as was thoroughly demonstrated in [23], this kind of $F(t)$ with a rather small value $\delta \equiv \Delta/T_c \approx 0.8$ takes the place for perfect YBCO films deposited on sapphire, while for another kind of substrates (MgO, LaAlO_3) the polynomial type of $F(t)$ dependence looks more appropriate. Our measurements of the $R_s(T)$ dependence performed on the quasi-single-crystalline YBCO films deposited on CeO_2 -buffered sapphire substrates by a use of the dc off-axis magnetron sputtering technique also demonstrate the exponential form of the surface resistance $R_s(T)$ at low temperatures (see the next Section), thus confirming the result of the work [23]. This result seems to be important for understanding the nature of superconducting state in HTS materials, as it indicates that at least in the case under study (YBCO films on sapphire) there is no pure gapless superconducting state, predicting by widely accepted for YBCO cuprate (both single crystals and thin films) the scenario of $d_{x^2-y^2}$ symmetry of the order parameter with nodes. The other important characteristic of superconducting state, which determines the microwave conductivity (2), (3) and the surface impedance (1), is the relaxation time $\tau(T)$ of normal carriers. Basing on the phenomenological analysis of numerous experimental data on $R_s(T)$ of HTS single crystals [3–7, 19–22] and thin films [17, 18, 23], it was shown that the most appropriate temperature dependence $\tau(T)$ has the form:

$$\tau(t) = \frac{\tau(0)}{1 + gt^m}, \quad (6)$$

where $g = \tau(0)/\tau(1) \gg 1$; $m = 3-5$. Eq. (6) describes the strong enhancement of the quasi-particle relaxation time $\tau(T)$ when temperature lowers below T_c and its saturation at low temperatures [4]. This type of the $\tau(T)$ -dependence is usually ascribed to combined effect of different scattering mechanisms: electron-impurity, electron-phonon, etc. An analysis of the experimental data on $R_s(T)$ in the most perfect HTS single crystals and thin films [3–7, 17–23] reveals that at low temperatures $\tau(T)$ can reach large enough values of order 10^{-11} – 10^{-10} s. The latter means in the GHz frequency range that usually used in microwave measurements the condition $\omega\tau(T) = 1$ can be met at $T < T_c$ and the frequency dependence of the quasi-particle conductivity, given within the phenomenological approach by Eqs. (2), (3), becomes essential. At not too high temperatures below T_c one usually has: $\sigma_1 \ll \sigma_2$. In this case, as it follows from (1)–(3), the surface resistance R_s and reactance X_s can be easily expressed in a convenient form through the real part of conductivity $\sigma_1(T, \omega)$ and ac penetration depth $\lambda(T, \omega)$:

$$R_s(T, \omega) = \frac{\mu_0^2 \omega^2}{2} \lambda^3(T) \sigma_1(T, \omega), \quad (7)$$

$$X_s(T, \omega) = \omega \mu_0 \lambda(T); \lambda(T, \omega) = \lambda_L(T) + \Delta \lambda^{qp}(T, \omega), \quad (8)$$

where $\lambda_L = m^* / \mu_0 n_s(T) e^2$ is the London penetration depth and $\Delta \lambda^{qp}(T, \omega)$ is an addition to the ac penetration depth due to the quasi-particle screening, which emerges at $\omega \tau(T) \geq 1$. One of the most interesting features, observed in microwave studies of perfect HTS cuprate single crystals and thin films, is the emergence of broad enough peaks on temperature dependences of the surface resistance $R_s(T)$ and conductivity $\sigma_1(T)$. Such kind of a nonmonotonous behavior of the $R_s(T)$ dependence, schematically shown in Fig. 1, is characterized by a shift of this broad peak position on the temperature scale to higher temperatures, when the frequency increases. In general, as it follows from (2), (7), this peak results from the temperature dependences of $n_N(t)$ and $\tau(T)$ and its maximum position T_p approximately corresponds to the condition $\omega \tau(T_p) = 1$ [4]. Addition of impurities increases the scattering rate and suppresses the peak, as it was shown both for YBCO single crystals and perfect epitaxial films [1,17]. Thus, to observe such a type of nonmonotonous behavior in the GHz frequency range one should have a highly perfect HTS cuprate material with a high value of quasi-particle relaxation time (at least $\sim 10^{-11}$ s, as it was mentioned above).

Despite the prevalence of phenomenological two-fluid approach to explanation of microwave properties of HTS it is not possible to understand all features and peculiarities of the microwave response in the cuprate materials and more deep insight based on microscopic theory is to be needed. First of all it concerns the

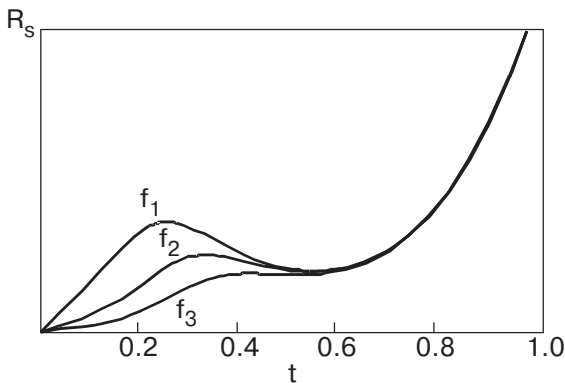


Fig. 1. Nonmonotonous surface temperature dependence of the resistance in perfect HTS single crystal (thin film) at different frequencies $f_1 < f_2 < f_3$. It is shown schematically; see, e.g. [4,17]. When frequency increases the peak smears while its position shifts to higher temperatures.

symmetry of order parameter, quasi-particle density, and relaxation time. For instance, recently it was shown that the quasi-particle relaxation rate $\tau^{-1}(T)$ exhibits a linear temperature dependence at low temperatures for different HTS cuprate single crystals ($\text{Bi}_2\text{Sr}_2\text{CaCu}_2\text{O}_{8+\delta}$, $\text{Tl}_2\text{Ba}_2\text{CuO}_{6+\delta}$, $\text{YBa}_2\text{Cu}_3\text{O}_{6.52}$) [9], which is consistent with the predictions of the microscopic theory [10] for the case of pure *d*-wave pairing with line nodes and weak elastic quasi-particle scattering. Detailed measurements of quasi-particle conductivity spectrum in Ortho-I $\text{YBa}_2\text{Cu}_3\text{O}_{6.993}$ and Ortho-II $\text{YBa}_2\text{Cu}_3\text{O}_{6.52}$ single crystals, performed by use of a novel broadband spectrometer in the range 1–21 GHz [8], have revealed that the microwave conductivity σ_1 differs from the simple Drude form (2) and obeys the empirical law:

$$\sigma_1^{(qp)}(\omega) = \frac{\sigma_1^{(qp)}(\omega \rightarrow 0)}{1 + (\omega \tau)^y}, \quad (9)$$

with the exponent $y \approx 1.67$ (for Ortho-I $\text{YBa}_2\text{Cu}_3\text{O}_{6.993}$) and $y \approx 1.45$ (for Ortho-II $\text{YBa}_2\text{Cu}_3\text{O}_{6.52}$). Such a difference of experimental $\sigma_1(\omega)$ dependence from that given by Drude law (2) points out that for analysis of these features one has to use more precise expression for microwave conductivity, e.g., that given by microscopic theory [10]:

$$\sigma^{(qp)}(T, \omega) = \frac{e^2}{m^*} \int_{-\infty}^{\infty} N(\varepsilon) \left(-\frac{\partial f}{\partial \varepsilon} \right) \frac{1}{[i\omega + \tau^{-1}(\varepsilon)]} d\varepsilon, \quad (10)$$

where $N(\varepsilon)$ is electron density of states; $f(\varepsilon)$ is the Fermi distribution function; $\tau(\varepsilon)$ is the energy-dependent quasi-particle relaxation time.

In what follows we demonstrate that peculiarities of the microwave surface resistance observed in our experiments performed on highly perfect quasi-single-crystalline YBCO films, deposited on CeO_2 -buffered sapphire substrates, can be explained on the base of Eq. (10) with additional assumptions about *s+id* type symmetry of the order parameter and the dominant role of extended *c*-oriented defects in quasi-particle scattering.

3. Experimental

Microwave measurements of YBCO films under study are performed by a use of two different techniques: a) coplanar resonator technique [25] which allows one to measure the surface resistance of films under study at frequencies $f = 5.25; 8; 17.75; 21$ GHz; b) an end-plate cavity resonator technique [24] which extends the frequency range to higher frequencies: $f = 34, 65, \text{ and } 134$ GHz. Several dc off-axis magnetron

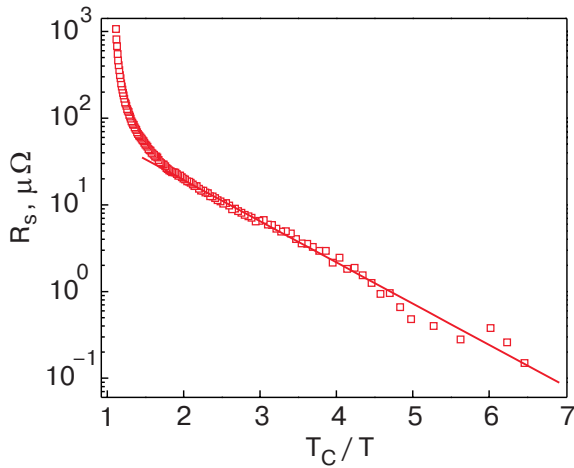


Fig. 2. $R_s(T)$ dependence of $\text{YBa}_2\text{Cu}_3\text{O}_{7-\delta}$ film on sapphire substrate measured by coplanar resonator technique at $f = 5$ GHz (semi-log scale). The straight line corresponds to the exponential temperature dependence of $R_s(T)$: $R_s(T) = R_{\text{res}} + R_0 \exp(-\Delta_s/T)$ with the small gap value $\Delta_s \approx 0.5T_c$ [23].

sputtered (OMS) as well as pulse laser deposited (PLD) YBCO films on CeO_2 -buffered r -cut single-crystal sapphire substrates have been measured in the temperature range 18–100 K. The film thickness is varied from 150 to 480 nm, and their structure and surface perfection is verified by x-ray diffractometry, TEM, HREM and AFM. The results of the microwave measurements are shown in Figs. 2–5. Fig. 2 demonstrates the $R_s(T)$ dependence for the OMS film measured at $f = 5$ GHz by a use of the coplanar resonator technique. The plot is shown in a semi-log scale vs. T_c/T . This distinctly indicates the exponential type of $R_s(T)$ dependence at low temperature with the energy gap value $\Delta_s/T_c \approx 0.5$. Such a result confirms the previous observation [23] which also demonstrated existence of a smaller gap ($\Delta_s \approx 0.8T_c$) in the quasi-particle spectrum for similar films. We suppose that evidence of the small gap in the $R_s(T)$ dependence (and, correspondingly, in the quasi-particle spectrum) is consistent with a scenario of the mixed ($s+id$ -type) electron pairing with the small admixture of s -wave component to the pure $d_{x^2-y^2}$ pairing, usually assuming for the perfect YBCO single crystals. This admixture [42,43] can arise because of enhanced (compared to that in single crystals) quasi-particle scattering due to the additional static disorder inherent to the films structure, such as: different growth-induced crystal structure defects of films [26–38] like internal low-angle boundaries, dislocations, stacking faults, twin boundaries, etc.

Figure 3 demonstrates the temperature dependence of ac penetration depth $\lambda(T)$, measured at several

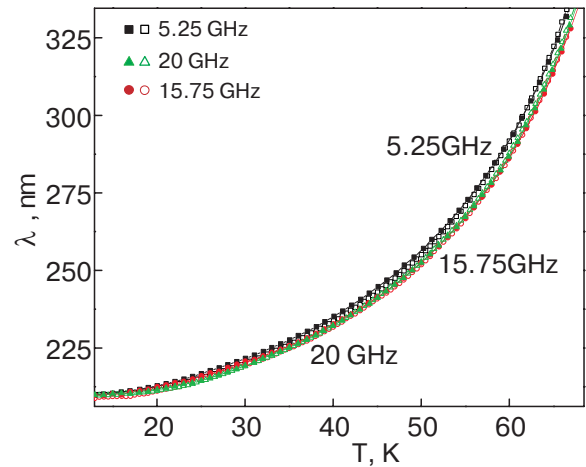


Fig. 3. The ac penetration depth $\lambda(T)$ measured by coplanar resonator technique at different frequencies $f = 5.25$; 17.25 and 21 GHz.

frequencies by a use of coplanar resonator technique. This dependence can be fitted well by an empirical law:

$$\lambda(T) = \frac{\lambda_0}{\sqrt{1 - t^n}}; \quad n > 2$$

For the most perfect quasi-single-crystalline OMS films the anomalous two-peak temperature dependences of the microwave surface resistance, $R_s(T)$, are observed at higher frequencies (see Figs. 4, 5) [24]. Microwave measurements in this case are performed with a use of cylindrical pure copper cavities 2, 4 and 8 mm in diameter. The film under study is exposed to the microwave field as one of the flat base of the copper cavity. The measurements are done using H_{011} mode at frequencies 134, 65, and 34 GHz. The OMS films with very smooth surface and the residual resistance at 20 K not higher than 6–8 mΩ revealed a distinct two-peak structure in the $R_s(T)$ dependence with peaks at 27–30 K and 48–51 K (Fig. 4). These

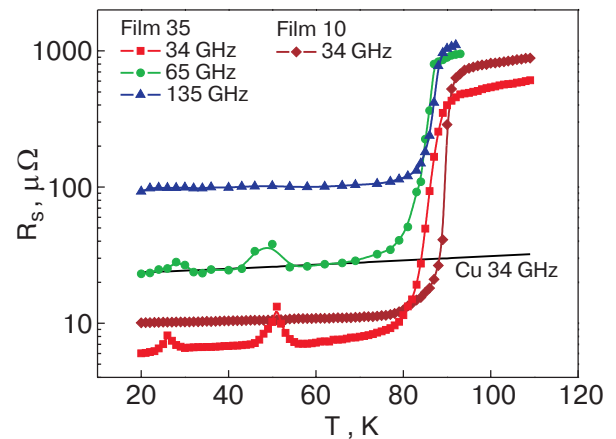


Fig. 4. $R_s(T)$ for two OMS films 35 and 10 at different frequencies. $R_s(T)$ for Cu is shown for comparison.

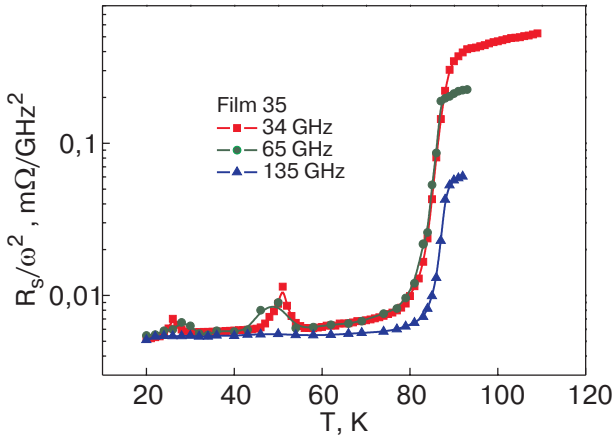


Fig. 5. $R_s(T)$ dependence for the perfect film 35 at three different frequencies normalized by ω^2 .

peaks become much more pronounced at the lowest frequency used in these experiments (34 GHz) and for thinner films, while their temperature positions remain almost unchanged. Figure 6 demonstrates that these peaks can be also seen in the $\lambda_{ac}(T)$ dependences. For less perfect (e.g., PLD) films, characterized by a higher density of linear defects, stacking faults, not so smooth surface, and much smaller size of the single-crystalline domains with disordered low-angle tilt boundaries, the $R_s(T)$ dependences appear to be monotonous and similar to those obtained in previous works [2,26,27]. The observed two-peak feature of $R_s(T)$ is believed to be an intrinsic microscopic feature of the most perfect quasi-single-crystalline YBCO films. This dependence differs from that of high quality YBCO single crystals, for which the sole peak in the $R_s(T)$ -dependence (see Fig. 1) was detected [1,4–6,17] but much broader one and strongly dependent upon the frequency of experiment. In Fig. 5 the two-peak dependences of $R_s(T)$ normalized by ω^2 for one of the most perfect YBCO film are presented at three different frequencies.

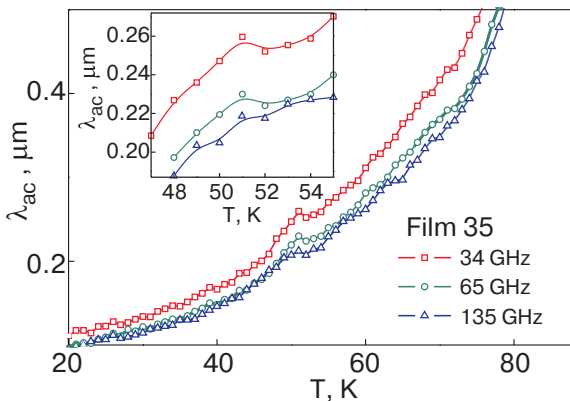


Fig. 6. Manifestation of the observed two-peak peculiarity in the ac penetration depth $\lambda(T)$ dependencies.

The substantial difference between $R_s(T)$ values of YBCO epitaxially grown highly biaxially-oriented films and YBCO single crystals is shown to exist, increasing with temperature, $T \rightarrow T_c$. One may suppose that this difference arises due to essentially different crystal defect structure in YBCO epitaxial films and single crystals.

Highly perfect quasi-single-crystalline $YBa_2Cu_3O_{7-\delta}$ films exhibit several times higher microwave surface resistance than perfect YBCO single crystals. A different dimensionality of crystal defects in YBCO single crystals and thin films probably is responsible for the difference. Two major types of crystal defects (point and planar ones, i.e., oxygen vacancies and twins) are known to be the most essential and defining YBCO single crystal electromagnetic behavior. In a contrary, linear defects are currently shown to be most important for the films. Despite the perfect crystallinity, different types of linear defects, e.g. dislocations, as well as dislocation arrays, have been identified by TEM/HREM in YBCO films. In order to understand the high-frequency electromagnetic behavior of YBCO films, the existence of arrays of edge dislocations in YBCO films should be taken into account, in particular, *out-of-plane edge dislocations*, associated with low-angle tilt dislocation boundaries. TEM/HREM/XRD/AFM characterization of the films under study revealed a smooth surface (peak-to-valley is 2 nm), high average in-plane density of out-of-plane edge dislocations ($10^{11} - 10^{10} \text{ cm}^{-2}$) and a large size of single-crystalline domains ($\langle D \rangle = 100 - 250 \text{ nm}$), which are separated by low-angle dislocation boundaries with in-plane misalignment of $1 - 2^\circ$ [26–31]. Linear defects, in particular, *out-of-plane edge* («threading») dislocations have been proven to play a remarkable role in the value and temperature dependence of the microwave surface resistance in epitaxial YBCO films due to extended stress-strain fields around a normal dislocation core. The contribution out-of-plane edge dislocation to the R_s increases with temperature due to the proximity effect. The area with suppressed superconducting order parameter can be estimated as about $8 \cdot 10^{-13} \text{ cm}^2$ per dislocation at 77 K [27].

4. Theoretical model

The value of microwave surface impedance $Z_s(T, \omega)$ in a linear regime at zero applied dc magnetic field is directly determined by the real part $\sigma_1(T, \omega)$ of high-frequency electron conductivity $\sigma(T, \omega) = \sigma_1(T, \omega) - i\sigma_2(T, \omega)$ of a superconductor (see Sec. 2, Eqs. (1)–(3), (7), (8)). Thus, the observed exponential low-temperature dependence and peaks on $R_s(T)$ dependence reveal also the temperature dependence of

$\sigma_1(T, \omega)$. Similarly, peaks in $X_s(T)$ and $\lambda(T)$ dependencies, accordingly to Eqs. (7) and (8), are related to contribution of the normal component of electron fluid. The $\sigma_1(T, \omega)$ value is generally ascribed to contribution of the «normal» component of electron fluid to the *ac* conductivity (Sec. 2). It should be mentioned that the phenomenological «two-fluid» model, which is frequently used for description of microwave properties of superconductors [1,3,4,17–23], also follows from the microscopic BCS theory. A very essential feature of the microscopic approach is that the role of normal component of electron fluid in superconductor is played by a gas of Bogolyubov quasi-particles, which are determined as a superposition of electron and hole states in a normal Fermi liquid. Due to this circumstance, the normal electron fluid in superconductors has quite different properties compared to that in a normal metal [39,40]. We will take into account the peculiarities of the «normal» electron fluid of Bogolyubov quasi-particles in superconductor and will show that the principal features of HTS microwave response, including the observed two peaks of $R_s(T)$ and $X_s(T)$ dependencies, can be qualitatively explained using the Boltzmann kinetic equation approach for Bogolyubov quasi-particles with certain additional assumptions about the symmetry of superconducting state in HTS and its dependence on the concentration of static defects (impurities, oxygen vacancies, dislocations, etc.). Namely, we will assume that the case of anisotropic $s + id$ pairing is realized [41–43] (see Fig. 7):

$$\Delta_{\mathbf{p}} = \Delta_0 + i\Delta_1 \cos(2\varphi), \quad \varphi = \arctan(p_y/p_x) \quad (11)$$

and the relation between isotropic Δ_0 and angle-dependent Δ_1 components of the pairing potential Δ_p ,

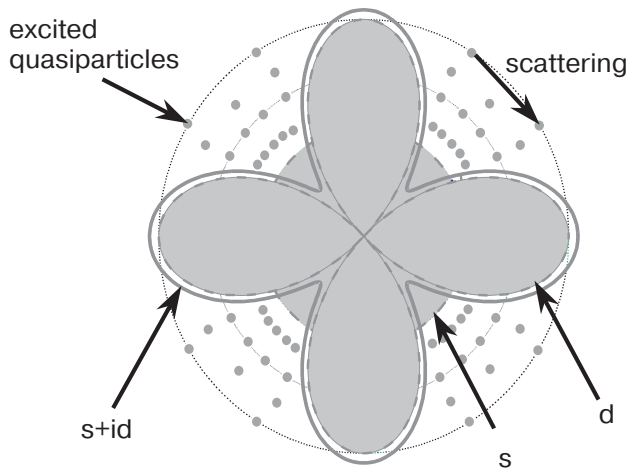


Fig. 7. Schematic representation of the order parameter anisotropy and quasi-particle scattering in the case of $s + id$ symmetry of Cooper pairing.

described by Eq. (11), is rather sensitive to the defect concentration and to different kind of borders (e.g., film surfaces and twin boundaries) [42,43].

In order to calculate the contribution of Bogolyubov quasi-particles to the conductivity value at microwave frequencies we will use the Boltzmann kinetic equation for nonequilibrium distribution function of quasi-particles $f(p)$. This approach is well known and was widely used for theoretical consideration of electron kinetic properties in normal metals [44]. Due to its relative simplicity it allows in principle to take into account peculiarities of electron spectrum and Fermi surface in HTS cuprates [45,46] as well as different mechanisms of electron scattering. This approach was argued on the base of the microscopic BCS theory in the quasi-classical limit for quasiparticles in superconducting state [47–49]. The Boltzmann equation in this case may be written in the form [47]:

$$\frac{\partial f}{\partial t} + v_g(\mathbf{p}) \frac{\partial f}{\partial \mathbf{r}} + e^*(\varepsilon_{\mathbf{p}}) E(\mathbf{r}, t) \frac{\partial f_0}{\partial \mathbf{p}} = \frac{f - f_0}{\tau(\varepsilon_p)}, \quad (12)$$

where $\varepsilon_{\mathbf{p}} = \sqrt{\xi_{\mathbf{p}}^2 + \Delta_{\mathbf{p}}^2}$ is the energy of quasi-particle; $\xi_{\mathbf{p}} = v_F(\mathbf{p} - \mathbf{p}_F)$ is the energy of a normal electron in a vicinity of the Fermi surface; \mathbf{v}_F and \mathbf{p}_F are the Fermi velocity and momentum, respectively; f_0 is the equilibrium Fermi distribution function of quasiparticles; $\mathbf{v}_g(\mathbf{p}) = \mathbf{v}_F(\mathbf{p})(\xi_p/\varepsilon_p)$ is the group velocity of quasiparticles, $e^*(\mathbf{p}) = e \cdot (\xi_{\mathbf{p}}/\varepsilon_{\mathbf{p}})$ is the quasiparticle charge (which is different from the normal electron charge e , because a Bogolyubov quasiparticle is a superposition of electron and hole states in the Fermi liquid [40]); $\tau(\varepsilon_{\mathbf{p}})$ is the relaxation time of quasiparticles, which in the case of elastic scattering by static defects can be calculated from the following well known expression [40,44]:

$$\tau^{-1}(\varepsilon_{\mathbf{p}}) = \frac{2\pi}{\hbar} \int |M_{\mathbf{p}, \mathbf{p}'}|^2 l^2(\mathbf{p}, \mathbf{p}') \delta(\varepsilon_{\mathbf{p}} - \varepsilon_{\mathbf{p}'}) \frac{d^3 p'}{(2\pi\hbar)^3}. \quad (13)$$

Integration in Eq. (13) is performed in the vicinity of the Fermi surface. $M_{\mathbf{p}, \mathbf{p}'}$ is the matrix element of electron scattering on the defect; $l(\mathbf{p}, \mathbf{p}')$ is the so-called «coherence factor»:

$$l^2(\mathbf{p}, \mathbf{p}') = 1 + \frac{\xi_{\mathbf{p}} \xi_{\mathbf{p}'} - \Delta_{\mathbf{p}} \Delta_{\mathbf{p}'}}{\varepsilon_{\mathbf{p}} \varepsilon_{\mathbf{p}'}} \quad (14)$$

which describes the difference between scattering of quasiparticles comparatively to usual electrons in the framework of BCS theory [40,44] and provides a strong dependence of the relaxation time on the quasiparticle energy even in the case of elastic scattering on static defects. In the case of isotropic s -wave

pairing and scattering on point-like defects this dependence can be estimated as [47]:

$$\tau_i(\varepsilon_{\mathbf{p}}) \approx \tau_n(\varepsilon_{\mathbf{p}}/\xi_{\mathbf{p}}). \quad (15)$$

So, $\tau_i(\varepsilon_{\mathbf{p}})$ diverges at the edge of the gap, when $p \rightarrow p_F$ and the group velocity v_g goes to zero. For the sake of simplicity we have assumed in Eq. (13) that all defects in the crystal lattice are identical and can be characterized by the same matrix element $M_{p,p'}$. If there are several sorts of scattering defects, e.g., point-like (oxygen vacancies) and extended ones (dislocations, twin boundaries) oriented along the c -axis, as they usually are in the case of cuprate epitaxial films and as it was discussed in the previous section, it follows from Eq. (13) that:

$$\tau^{-1}(\varepsilon_{\mathbf{p}}) \approx \tau_i^{-1}(\varepsilon_{\mathbf{p}}) + \tau_{\text{ext}}^{-1}(\varepsilon_{\mathbf{p}}). \quad (16)$$

The energy dependences of the relaxation rates in the right hand side of Eq. (16) for point-like and extended defects may be quite different because point like defects can scatter electrons in all directions of the momentum space, while scattering on extended defects can proceed only with a conservation of momentum along the c -axis. This becomes especially important for layered HTS materials, where electrons move mainly within CuO_2 layers. In the case of d -wave or assumed $s + id$ (or other type) anisotropic pairing, an additional strong dependence of the relaxation time on the quasi-particles energy $\varepsilon_{\mathbf{p}}$ has to appear due to a confinement of momentum space, where the quasi-particles can be scattered, with a decrease of $\varepsilon_{\mathbf{p}}$. This effect follows directly from Eq. (13) due to the δ -function term in the integrand. In a certain sense, this effect can be considered as an analog of Andreev reflection of quasi-particle in the momentum space (Fig. 7). The confinement of momentum space for quasi-particles scattering is mostly essential for the scattering on extended defects, leading to a very rapid increase of $\tau_{\text{ext}}(\varepsilon_{\mathbf{p}})$, when $\varepsilon_{\mathbf{p}}$ decreases and approaches the value Δ_{max} ($\Delta_{\text{max}} = \max(\Delta_{\mathbf{p}})$), or correspondingly Δ_{min} ($\Delta_{\text{min}} = \min(\Delta_{\mathbf{p}})$), as it is shown in Fig. 7:

$$\tau_{\text{ext}}^{-1}(\varepsilon_{\mathbf{p}}) \propto \arcsin\left(\frac{\varepsilon_{\mathbf{p}}}{\Delta_{\text{max}(\text{min})}}\right). \quad (17)$$

The general solution for the quasi-particles ac conductivity can be obtained from Eq. (12) in the usual manner [44,50]. The real part $\sigma_1(T, \omega)$ can be written in the form

$$\sigma_1(T, \omega) = \int \frac{e^2 v_g^2(\varepsilon_{\mathbf{p}}) \tau(\varepsilon_{\mathbf{p}})}{1 + \omega^2 \tau^2(\varepsilon_{\mathbf{p}})} \left(-\frac{\partial f_0}{\partial \varepsilon}\right) \frac{d^3 p}{(2\pi\hbar)^3}, \quad (18)$$

which is quite similar to that given by the microscopic theory [10] (see Eq.(10)).

A strong temperature dependence of $\sigma_1(T, \omega)$ as well as its frequency dependence arise usually due to the $(-\partial f_0/\partial \varepsilon)$ term in the integrand of Eq. (18). Quite formally this solution can be rewritten in the Drude-like form:

$$\sigma_1(T, \omega) = \frac{n_n(T)e^2}{m} \left\langle \frac{\tau(\varepsilon_{\mathbf{p}})}{1 + \omega^2 \tau^2(\varepsilon_{\mathbf{p}})} \right\rangle_T, \quad (19)$$

where $n_n(T)$ is the effective concentration of thermally excited quasiparticles, $\langle \dots \rangle_T$ denotes thermal averaging. As it was originally supposed in [4,5,8], the nonmonotonous character and peak dependence of $R_s(T)$ as well as its frequency dependence can be explained properly by a strong increase of quasi-particle relaxation time with temperature lowering, accordingly to the Drude expression (2) for the ac conductivity $\sigma_1(T, \omega)$. The peak position corresponds to the condition $\tau^{-1} \approx \omega$. We suppose that this explanation is valid also in our case, when two peaks are observed. The emergence of two peaks instead of one can be explained by existence of two different Δ_{max} and Δ_{min} values for the assumed case of $s + id$ pairing (see Fig. 7), while the sharpness of these peaks comparatively to the peak in single crystals is determined by a very strong energy dependence (with an infinite slope of derivative $\partial \tau/\partial \varepsilon$ at $\varepsilon = \Delta_{\text{max}(\text{min})}$) of the relaxation time (Eq. (17)), when quasiparticles are scattered preferably by extended defects. This strong energy dependence of $\tau_{\text{ext}}(\varepsilon)$ after thermal averaging transforms into sharp peaks of $\sigma_1(T)$ accordingly to Eq. (19).

The present model can explain also some additional features of the microwave response of YBCO films under study, such as: (i) smearing of peaks with the frequency increase or decrease; (ii) lowering of $R_s(T)$ and smearing of peaks with an increase of point-like defect concentration.

5. Discussion

The obtained results shown in Figs. 2–6, namely: the exponential law for $R_s(T)$ at low temperatures and nonmonotonous two-peak structure of $Z_s(T, \omega)$ in perfect single-crystalline YBCO epitaxial films on sapphire, give a strong argument in favor of anisotropic electron pairing in HTS (preferably, of the $s+id$ type, at least for our films). The two-peak peculiarity of $Z_s(T)$ dependence for the most perfect single-crystalline YBCO films observed for the first time in [24], as well as the difference from

nonmonotonous $Z_s(T, \omega)$ dependence for perfect single crystals (and also some less perfect films), can be explained, using just two assumptions: (i) the anisotropic $s+id$ character of electron pairing, and (ii) the dominant role of extended c -oriented defects in electron scattering processes. These assumptions look quite natural with regard to thin films, where surfaces and/or twin boundaries can lead to more complicated character of electron pairing than the pure d -wave pairing in perfect single crystals [42,43]. On the other hand, the extended c -oriented linear or planar defects (most probably, out-of-plane edge dislocations and twins) can play a dominant role in electron scattering. In the case of untwinned single crystals there are no extended defects. Therefore, only point defects are essential for electron scattering at low temperatures. The above two assumptions, which seem to be specific for thin films, make a difference from single crystals and, thus, provide the difference in microwave response: one broad peak of $R_s(T)$ for single crystals and two sharp peaks for perfect films. For less perfect films with a larger number of point-like defects the extended c -oriented defects don't play significant role in quasiparticles scattering. In this case the films properties at microwave frequencies should be rather similar to that of single crystals.

The observed two peaks of $R_s(T)$ are much more narrow compared with a single peak, observed in perfect single crystals due to quite different defect structures in films and single crystals, as it was discussed above. Namely, a large number of extended defects together with an anisotropic pairing can lead to the emergence of a sharp peak at $T \sim \Delta_{\max}(T)$ (or $\Delta_{\min}(T)$), as it follows from Eq. (19). The second peak at a lower temperature is caused by the anisotropy of pairing potential (existence of two different extreme values Δ_{\max} and Δ_{\min} for different directions in the momentum space (as it is shown schematically in Fig. 7)). The present model for quasiparticles conductivity also allows to understand the frequency dependence of the observed peculiarities and their smearing, when the number of point-like defects increases, thus leading to an increase of $\tau_i^{-1}(\epsilon_p)$. It should be noted that in contrast to suggestions made in some theoretical works, it does not seem to be necessary to take into account a contribution of inelastic quasiparticles scattering by collective excitations (magnons, phonons, etc.). The two-peak temperature dependence of $\sigma_1(T, \omega)$ can occur in accordance to Eq. (19) even in the case of elastic scattering by extended static defects due to an additional effect of anisotropy (caused by or anisotropic $s + d$ or $s + id$ wave pairing), which leads to

confinement of the momentum space available for scattered quasiparticles, as it was mentioned above.

6. Conclusion

The observed two-peak character of $R_s(T)$ dependence is a feature of the most perfect quasi-single-crystalline YBCO films, characterized by a smooth surface, low concentration of defects, large domain size and low-angle boundaries between domains. We suppose that the main reason for observation of this effect in our highly perfect films (as well as its absence in less perfect films or single crystals) is a rather low density of point-like defects comparatively to the density of extended defects (such as edge dislocations or twin planes, parallel to the c -axis). This condition is not fulfilled in untwinned single crystals or less perfect (e.g., PLD) films, where point defects play the major role in quasiparticles scattering, and $R_s(T)$ dependence is monotonous or exhibits a single broad maxima. Thus, we suppose that the two-peak character of $R_s(T)$, observed experimentally for the first time in our work [24], is an intrinsic fundamental property and reveals the peculiarities of anisotropic electron pairing and quasiparticle scattering by extended defects parallel to the c -axis. We suppose also that this effect, as well as the difference from the case of single crystals and less perfect films, can be properly described using the Boltzmann kinetic equation approach for Bogolyubov quasi-particles.

This work was supported by the National Academy of Sciences of Ukraine through the Institute for Metal Physics by the theme No. 0036 and by the Science & Technology Center in Ukraine through the Project No. 3022.

1. D.A. Bonn, S. Kamal, K. Zhang, R. Liang, D.J. Baar, E. Klein, and W.N. Hardy, *Phys. Rev.* **B50**, 4051 (1994).
2. S. Hensen, G. Muller, C.T. Rieck, and K. Scharnberg, *Phys. Rev.* **B56**, 6237 (1997).
3. M.R. Trunin, *J. Superconductivity* **11**, 381 (1998).
4. A. Hosseini, R. Harris, S. Kamal, P. Dosanjh, J. Preston, R. Liang, W.N. Hardy, and D.A. Bonn, *Phys. Rev.* **B60**, 1349 (1999).
5. A.J. Berlinsky, D.A. Bonn, R. Harris, and C. Kallin, *Phys. Rev.* **B61**, 9088 (2000).
6. M.I. Tsindlekht, E.B. Sonin, M.A. Golosovsky, D. Davidov, X. Castel, M. Guilloux-Viry, and A. Perin, *Phys. Rev.* **B61**, 1596 (2000).
7. R. Harris, A. Hosseini, S. Kamal, P. Dosanjh, R. Liang, W.N. Hardy, and D.A. Bonn, *Phys. Rev.* **B64**, 064509 (2001).
8. P.J. Turner, R. Harris, S. Kamal, M.E. Hayden, D.M. Broun, D.C. Morgan, A. Hosseini, P. Dosanjh,

- G. Mullins, J.S. Preston, R. Liang, D.A. Bonn, and W.N. Hardy, *Phys. Rev. Lett.* **90**, 237005 (2003).
9. S. Ozcan, P.J. Turner, J.R. Waldram, R.J. Drost, P.H. Kes, and D.M. Broun, *cond-mat/0508621*, v. 1 (2005).
10. P.J. Hirschfeld, W.O. Putikka, and D.J. Scalapino, *Phys. Rev. Lett.* **71**, 3705 (1993); *Phys. Rev.* **B50**, 10250 (1994).
11. C.T. Rieck, K. Scharnberg, and J. Ruvalds, *Phys. Rev.* **B60**, 12432 (1999).
12. M.H. Hettler and P.J. Hirschfeld, *Phys. Rev.* **B61**, 11313 (2000).
13. D. Duffy, P.J. Hirschfeld, and D.J. Scalapino, *Phys. Rev.* **B64**, 224522 (2001).
14. W.A. Atkinson and P.J. Hirschfeld, *Phys. Rev. Lett.* **88**, 187003 (2002).
15. A.C. Durst and P.A. Lee, *Phys. Rev.* **B65**, 094501 (2002).
16. D.E. Sheehy, *Phys. Rev.* **B68**, 054529 (2003).
17. J. Einfeld, P. Lahl, R. Kutzner, R. Wordenweber, and G. Kastner, *Physica* **C351**, 103 (2001).
18. I. Vendik, *Supercond. Sci. Technol.* **13**, 974 (2000).
19. H.J. Fink, *Phys. Rev.* **B58**, 9415 (1998); *ibid.* **61**, 6346 (2000).
20. M.R. Trunin, *JETP Lett.* **72**, 583 (2000).
21. M.R. Trunin, Yu.A. Nefyodov, and H.J. Fink, *JETP* **91**, 801 (2000).
22. H.J. Fink and M.R. Trunin, *Phys. Rev.* **B62**, 3046 (2000).
23. M. Hein, T. Kaiser, and G. Muller, *Phys. Rev.* **B61**, 640 (2000).
24. V.M. Pan, A.L. Kasatkin, V.A. Komashko, A.A. Kalenyuk, C.G. Tretiatchenko, A.N. Ivanyuta, G.A. Melkov, *Proc. EUCAS'03*, 2187 (2004); *cond-mat/0404523*, v. 1 (2004); *J. Supercond.: Incorp. Magn.* (to be published).
25. M.J. Lancaster, *Passive Microwave Device Application of High-Temperature Superconductors*, Cambridge Univ. Press, Cambridge (1997).
26. V.M. Pan, V.S. Flis, V.A. Komashko, O.P. Karasevskaya, V.L. Svetshnikov, M. Lorenz, A.N. Ivanyuta, G.A. Melkov, E.A. Pashitskii, and H.W. Zandbergen, *IEEE Trans. Appl. Supercond.* **11**, 3960 (2001).
27. V.M. Pan, C.G. Tretiatchenko, V.S. Flis, V.A. Komashko, E.A. Pashitskii, A.N. Ivanyuta, G.A. Melkov, W.H. Zandbergen, and V.L. Svetshnikov, *J. Supercond.: Incorp. Magn.* **16**, 889 (2003).
28. S.K. Streiffer, B.M. Lairson, C.B. Eom, B.M. Clemens, J.C. Bravman, and T.H. Geballe, *Phys. Rev.* **B43**, 13007 (1991).
29. Y. Gao, K.L. Merkle, G. Bai, H.L. Chang, and D.J. Lam, *Physica* **C174**, 1 (1991).
30. S.J. Pennycook, M.F. Chisholm, D.E. Jesson, R. Feenstra, S. Zhu, X.Y. Cheng, and D.J. Lowndes, *Physica* **C202**, 1 (1992).
31. V.L. Svetshnikov, V.M. Pan, Ch. Traeholt, and W.H. Zandbergen, *IEEE Trans. Appl. Supercond.* **7**, 1396 (1997).
32. B. Dam, J.M. Huijbregtse, F.C. Claassen, R.C.F. van der Geest, G. Doornbos, J.H. Rector, A.M. Testa, S. Freisem, J.C. Martinez, B. Stauble-Pumpin, and R. Griessen, *Nature (London)* **399**, 439 (1999).
33. J.M. Huijbregtse, B. Dam, R.C. F. van der Geest, F.C. Klaassen, R. Elberse, J.H. Rector, and R. Griessen, *Phys. Rev.* **B62**, 1338 (2000).
34. B. Dam, J.M. Huijbregtse, and J.H. Rector, *Phys. Rev.* **B65**, 064528 (2002).
35. Casaca, G. Bonfait, C. Dubourdieu, F. Weiss, and J.P. Senateur, *Phys. Rev.* **B59**, 1538 (1999).
36. S. Berger, D.-G. Crete, J.-P. Contour, K. Bouzehouane, J.-L. Maurice, and O. Durand, *Phys. Rev.* **B63**, 144506 (2001).
37. L.X. Cao, T.L. Lee, F. Renner, Y.X. Su, R.L. Johnson, and J. Zegenhagen, *Phys. Rev.* **B65**, 113402 (2002).
38. J.J. Robles, A. Bartaszyte, H.P. Ng, A. Abrutis, and F. Weiss, *Physica* **C400**, 36 (2003).
39. G.E. Blonder, M. Tinkham, and T.M. Klapwijk, *Phys. Rev.* **B25**, 4515 (1982).
40. M. Tinkham, *Introduction to Superconductivity* McGraw-Hill, Inc., New York (1996).
41. D.J. Scalapino, *Phys. Rep.* **250**, 329 (1995).
42. J.Y.T. Wei, N.C. Yeh, D.F. Garrigus, and M. Strasik, *Phys. Rev. Lett.* **81**, 2542 (1998).
43. C.G. Tsuei and J.R. Kirtley, *Rev. Mod. Phys.* **72**, 969 (2000).
44. A.A. Abrikosov, *Fundamentals of the Theory of Metals*, Elsevier Science, Amsterdam (1988).
45. M.C. Schabel, C.-H. Park, A. Matsuura, Z.-X. Shen, D.A. Bonn, R. Liang, and W.N. Hardy, *Phys. Rev.* **B57**, 6090 (1998).
46. T. Jarlborg and G. Santi, *Physica* **C329**, 243 (2000).
47. A.G. Aronov, Yu.M. Galperin, V.L. Gurevich, and V.I. Kozub, in: *Nonequilibrium Superconductivity*, D.N. Langenberg and A.I. Larkin (eds.), Elsevier Science Publishers B.V., Amsterdam (1986), p. 325; *Adv. Phys.* **30**, 539 (1981).
48. G. Blatter, V.B. Geshkenbein, and N.B. Kopnin, *Phys. Rev.* **B59**, 14663 (1999).
49. N.B. Kopnin, *J. Low Temp. Phys.* **124**, 209 (2001).
50. J.M. Ziman, *Principles of the Theory of Solids*, University Press, Cambridge (1972).